

SRAO CO Observation of 11 Supernova Remnants in $l = 70^\circ$ to 190°

Il-Gyo Jeong¹ • Do-Young Byun^{2,3} •
Bon-Chul Koo¹ •
Jea-Joon Lee, Jung-Won Lee, Hyunwoo Kang²

Abstract We present the results of $^{12}\text{CO } J = 1-0$ line observations of eleven Galactic supernova remnants (SNRs) obtained using the Seoul Radio Astronomy Observatory (SRAO) 6-m radio telescope. The observation was made as a part of the SRAO CO survey of SNRs between $l = 70^\circ$ and 190° , which is intended to identify SNRs interacting with molecular clouds. The mapping areas for the individual SNRs are determined to cover their full extent in the radio continuum. We used half-beam grid spacing ($60''$) for 9 SNRs and full-beam grid spacing ($120''$) for the rest. We detected CO emission towards most of the remnants. In six SNRs, molecular clouds showed a good spatial relation with their radio morphology, although no direct evidence for the interaction was detected. Two SNRs are particularly interesting: G85.4+0.7, where there is a filamentary molecular cloud along the radio shell, and 3C434.1, where a large molecular cloud appears to block the western half of the remnant. We briefly summarize the results obtained for individual SNRs.

Keywords supernova remnants — ISM: molecules — ISM: clouds

Il-Gyo Jeong

Astronomy Program, Department of Physics and Astronomy,
Seoul National University, Seoul 151-742, Republic of Korea

Do-Young Byun

Korea Astronomy & Space Science Institute, Daejeon 305-348,
Republic of Korea

Yonsei University Observatory, Yonsei University, Seongsan-ro
262, Seodaemun, Seoul 120-749, Republic of Korea

Bon-Chul Koo

Astronomy Program, Department of Physics and Astronomy,
Seoul National University, Seoul 151-742, Republic of Korea

Jea-Joon Lee, Jung-Won Lee, Hyunwoo Kang

Korea Astronomy & Space Science Institute, Daejeon 305-348,
Republic of Korea

1 Introduction

Supernova (SN) explosions are one of the most energetic events that can occur in a galaxy. SN explosions strongly modify the environment, and at the same time, the evolution of a supernova remnant (SNR) is governed primarily by the environment itself. As stars are formed due to the gravitational collapse of molecular clouds, there is a large possibility that a SN explodes adjacent to its parental molecular cloud (MC). Thus, an environment with molecular clouds may not be unusual during a SNR evolution.

There are indeed SNRs that show direct evidence of SNR interaction with molecular clouds (e.g., see Koo 2003; Jiang et al. 2010). IC443 is a prototypical object from which high-velocity, broad emission lines from shocked atomic and molecular gases have been detected (DeNoyer 1979; Snell et al. 2005; Lee et al. 2008, 2012, and references therein). Shock-excited infrared emission lines from H_2 and other molecules have been detected as well. On the other hand, it is proposed that centrally enhanced thermal X-ray emissions or the spatial coincidence of molecular clouds can serve as an indirect indication of SNR-MC interaction. SNR 3C391 belongs to this category, having break-out morphology in radio emission (Reach et al. 1999; Chen et al. 2004).

SNR-MC interactions have several important astrophysical implications. Strong SNR shocks interacting with molecular clouds may produce high-energy gamma-ray emission due to enhanced pion decay emission from the collision of cosmic ray protons accompanied with efficient kinematic energy conversion in a dense molecular environment. The gamma-ray emission detected towards the SNRs CTB 37B, IC 443, and W51C indeed show an extended spatial distribution coincident with dense molecular clouds (Aharonian et al. 2008; Acciari et al. 2009; Abdo et al. 2009). This could be the first direct evidence for the production of cosmic

Table 1 List of Supernova Remnants between $l=70^\circ$ and 190°

Galactic Coordinates	Name(s)	α (J2000) (h m s)	δ (2000) ($^\circ$ $'$)	Size (arcmin)	Type ^a	CO ^b Observation
73.9 +0.9		20 14 15	+36 12	22?	S?	This paper
74.0 -8.5	Cygnus Loop	20 51 00	+30 40	230×160	S	—
74.9 +1.2	CTB87	20 16 02	+37 12	8×6	F	4
76.9 +1.0		20 22 20	+38 43	12×9	?	This paper
78.2 +2.1	γ Cygni SNR	20 20 50	+40 26	60	S	1, 5
82.2 +5.3	W63	20 19 00	+45 30	95×65	S	1
84.2 -0.8		20 53 20	+43 27	20×16	S	This paper, 6
84.9 +0.5 ^c		20 50 30	+44 53	6	S	—
85.4 +0.7		20 50 40	+45 22	24	S	This paper
85.9 -0.6		20 58 40	+44 53	24	S	This paper
89.0 +4.7	HB21	20 45 00	+50 35	120×90	S	1, 2
93.3 +6.9	DA530	20 52 25	+55 21	27×20	S	This paper
93.7 -0.2	CTB104A	21 29 20	+50 50	80	S	3
94.0 +1.0	3C434.1	21 24 50	+51 53	30×25	S	This paper
106.3 +2.7		22 27 30	+60 50	60×24	?	3, 7
109.1 -1.0	CTB109	23 01 35	+58 53	28	S	3, 8
111.7 -2.1	Cassiopeia A	23 23 26	+58 48	5	S	3
114.3 +0.3		23 37 00	+61 55	90×55	S	3
116.5 +1.1		23 53 40	+63 15	80×60	S	3
116.9 +0.2	CTB 1	23 59 10	+62 26	34	S	1, 3
119.5 +10.2	CTA 1	00 06 40	+72 45	90?	S	1
120.1 +1.4	Tycho	00 25 18	+64 09	8	S	3
126.2 +1.6		01 22 00	+64 15	70	S?	3
127.1 +0.5	R5	01 28 20	+63 10	45	S	3
130.7 +3.1	3C58	02 05 41	+64 49	9×5	F	3
132.7 +1.3	HB3	02 17 40	+62 45	80	S	1, 3
156.2 +5.7		04 58 40	+51 50	110	S	1
160.9 +2.6	HB9	05 01 00	+46 40	140×120	S	1
166.0 +4.3	VRO 42.05.01	05 26 30	+42 56	55×35	S	1
166.2 +2.5 ^c	OA 184	05 19 00	+41 55	90×70	S	This paper
179.0 +2.6		05 53 40	+31 05	70	S?	This paper
180.0 -1.7	S147	05 39 00	+27 50	180	S	This paper
182.4 +4.3		06 08 10	+29 00	50	S	This paper
184.6 -5.8	Crab Nebula	05 34 31	+22 01	7×5	F	—
189.1 +3.0	IC443	06 17 00	+22 34	45	C	3, 9

^aType of the SNR (S: Shell, F: Filled-Centre, C: Composite) (Green 2004)^bReferences are: (1) Byun (2004), (2) Byun et al. (2006), (3) FCRAO Survey (Taylor et al. 2003), (4) Kothes et al. (2003), (5) Higgs et al. (1983), (6) Feldt & Green (1993), (7) Kothes et al. (2001b), (8) Sasaki et al. (2006), (9) Snell et al. (2005).^cG84.9+0.5 and G166.2+2.5 (OA184) have been identified as HII regions (Foster et al. 2006, 2007) and removed in the Green's 2009 catalog.*Note:* The parameters of the SNRs are from the Green's 2004 catalog (Green 2004).

Table 2 Mapping Parameters of SNRs

Galactic Coordinates	Name(s)	Size (arcmin)	Observed area (arcmin)	Grid spacing (arcsec)
73.9 +0.9		22?	53×41	60
76.9 +1.0		12×9	17×18	60
84.2 -0.8		20×16	33×27	60
85.4 +0.7		24	51×61	60
85.9 -0.6		24	37×40	60
93.3 +6.9	DA530	27×20	37×36	60
94.0 +1.0	3C434.1	30×25	42×39	60
166.2 +2.5	OA184	90×70	97×94	60
179.0 +2.6		70	108×130	120
180.0 -1.7	S147	180	252×274	120
182.4 +4.3		50	63×61	60

ray protons by SNR shocks. The shocked, dense molecular gas could provide a physical condition for maser emission, e.g., 1720-MHz maser line (${}^2\Pi_{3/2}$, $J = \frac{3}{2}$, $F = 2 \rightarrow 1$) of the OH molecule. From SNRs W28, W44, and IC443, OH maser emissions were detected behind the leading edge of the shock (Claussen et al. 1997), and according to theoretical calculations (Elitzur 1976; Lockett et al. 1999; Wardle 1999), the masers arise only in slow, non-dissociative C -shocks with a large OH column density, which can be met only when the shock is observed tangentially (see the review by Wardle, M., & Yusef-Zadeh 2002).

About 270 SNRs are known in our Galaxy (Green 2009), and presently, about 20% – 30% of them are known to be interacting with molecular clouds (Jiang et al. 2010). However, insufficient effort has been made to conduct systematic searches. Huang & Thaddeus (1986) studied a molecular environment of galactic SNRs in $l = 70^\circ$ to 210° . However, due to the insufficient angular resolution ($\sim 8'.7$) of the telescope, the results were only useful for studying the distributions of large molecular cloud complexes near SNRs. More recently, large-scale CO surveys of the galactic plane have been conducted such as the Outer Galaxy Survey ($l = 102^\circ.5 - 141^\circ.5$) or the Galactic Ring Survey using the 14-m telescope of the Five College Radio Astronomy Observatory with an FWHM of $50''$ (Taylor et al. 2003; Jackson et al. 2006). There have been studies on individual SNRs in this survey area; however, no systematic studies have been conducted.

On the basis of the above background, we decided to carry out a systematic CO study of SNRs using the Seoul Radio Astronomy Observatory (SRAO) 6-m telescope. We limited the targets to the SNRs in $l = 70^\circ$ to 190° . The targets in the inner galaxy were excluded because of the ambiguity in determining the association. We observed most of the SNRs listed the Green’s 2004 catalog (Green 2004). Some results of

the survey were reported previously by Byun (2004) and Byun et al. (2006). They observed 9 SNRs having bright X-ray emissions and large angular sizes. They detected broad-line CO emissions from two SNRs (HB 21 and HB 3) and also found a morphological correlation between the CO and radio continuum distribution for two other SNRs (γ -Cygni and HB 9). For the remaining five SNRs, no evidence of SNR-MC interaction was observed. In this paper, we present the results obtained for eleven other SNRs.

This paper is organized as follows. In § 2, the observation details and target selection are explained. In § 3, the results for individual SNRs are presented. Section 4 summarizes the main results of this paper.

2 Observations

${}^{12}\text{CO } J=1-0$ (115.271204 GHz) observations were carried out from October 2003 to May 2005 using SRAO 6-m telescope. The telescope has an FWHM beam size of $120''$ and a main beam efficiency of 0.70 at 115 GHz (Koo et al. 2003). We used a 100 GHz SIS mixer receiver with a single-side band filter (Lee et al. 2002) and a 1024-channel auto-correlator with 50 MHz bandwidth, corresponding to a velocity coverage of 130 km s^{-1} (Choi et al. 2003). The system temperature ranged from 500 to 800 K depending on the elevation and weather conditions. Typical *rms* noise level on T_{mb} scale was $\sim 0.3 \text{ K}$ at a 1 km s^{-1} velocity resolution. In order to check the system performance, we regularly observed the bright standard source near the target at one or two hour intervals. Pointing accuracy was better than $20''$. The data were reduced by using the CLASS¹ software in the Gildas package developed by IRAM.

The targets were selected as follows. First, the Galactic longitudes of the SNRs are limited to $l = 70^\circ$ to 190° . Toward the inner Galactic region, many clouds are superposed along the line-of-sight, and hence, it is difficult to confirm the association of SNRs with molecular clouds. On the other hand, the SNRs beyond 190° are at low declinations due to which we have a rather limited observing time for them. According to the Green’s SNR catalog (Green 2004), there are 35 SNRs in this longitude range, and they are listed in Table 1². Second, the angular sizes of the SNRs are limited to $\geq 10'$ and $\leq 180'$, considering the beam size of the SRAO 6-m telescope. If the angular size is excessively small,

¹<http://www.iram.fr/IRAMFR/GILDAS>

²In the Green’s 2009 catalog (Green 2009), the number has increased to 37.

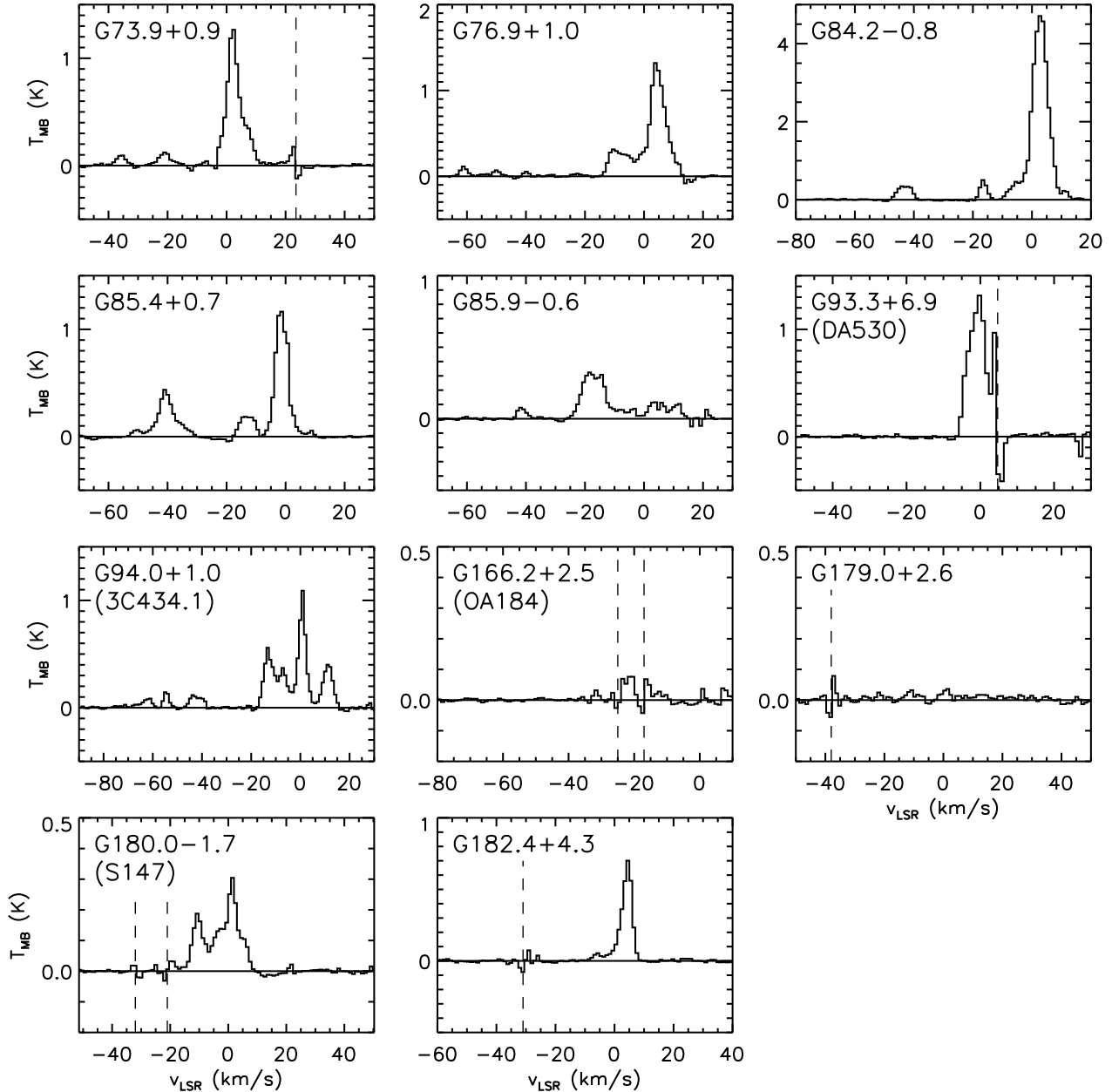


Fig. 1 Average $^{12}\text{CO } J = 1-0$ spectra of 11 supernova remnants. The dashed lines mark the telluric CO line positions.

the morphological comparison between the SNR and the molecular cloud becomes difficult, whereas if it is excessively large, the observation becomes highly time-consuming. Third, the SNRs in the area considered by the Five College Radio Astronomy Observatory Outer Galaxy Survey (FCRAO OGS) are excluded because the survey was performed with an adequate angular resolution ($60''$) and sensitivity. The FCRAO OGS survey covered the region $102^{\circ}.5 < l < 141^{\circ}.5$ and $-3^{\circ} < b < 5^{\circ}.4$ (Taylor et al. 2003). Finally, we excluded the SNRs observed by previous SRAO $^{12}\text{CO } J = 1-0$ observations

(Byun 2004, Byun et al. 2006). In the last column of Table 1, we list the references on the CO observations of individual SNRs.

The mapping areas for the individual SNRs are determined to cover their full extents in the radio continuum. Nine SNRs were observed with half-beam grid spacing ($60''$), whereas the two remaining SNRs were observed with full-beam grid spacing ($120''$) via the position switching mode. Table 2 lists the observed areas and the grid spacings for the target SNRs. The total number of spectra obtained in this study is ~ 45000 .

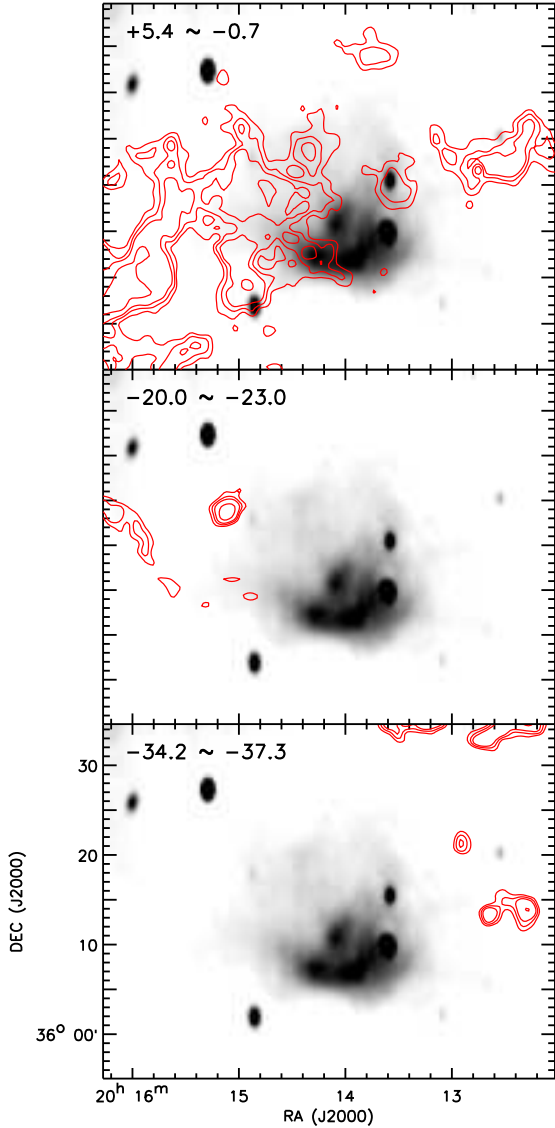


Fig. 2 $^{12}\text{CO } J = 1-0$ average intensity maps of G73.9+0.9 (contour levels: 1.2, 1.6, 2, 3 K). The gray-scale image is the Canadian Galactic Plane Survey (CGPS) 1420 MHz radio continuum image (scale range: 11~21 K) (Taylor et al. 2003).

3 Results

Figure 1 shows the average spectra toward 11 SNRs. Strong CO emission lines are detected toward all SNRs other than G166.2+2.5 and G179.0+2.6. In the following subsections, we summarize the results obtained for individual SNRs.

3.1 G73.9+0.9

G73.9+0.9 is located in the complex Cygnus area in the sky. This source has a faint and broad, spur-like struc-

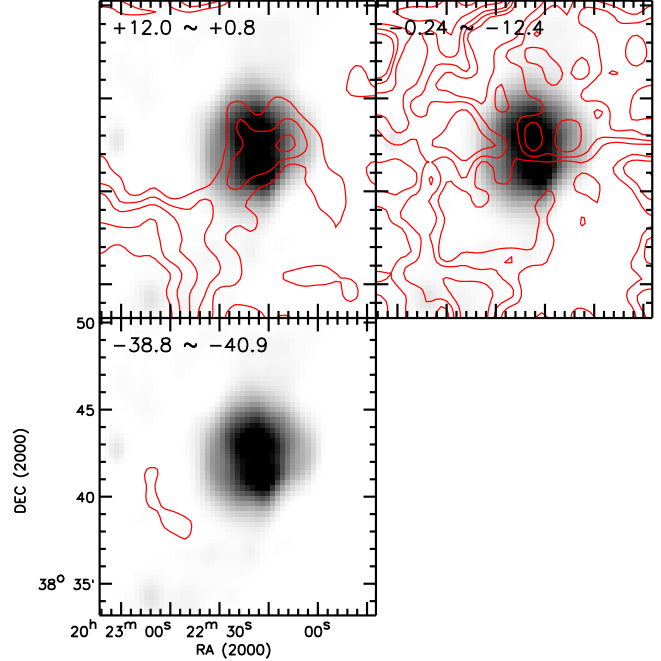


Fig. 3 $^{12}\text{CO } J = 1-0$ average intensity maps of G76.9+1.0 (contour levels: 0.5, 0.8, 1.2, 2, 3 K). The gray-scale image is the CGPS 1420 MHz radio continuum image (scale range: 11~21 K).

ture in radio and is classified as an SNR on the basis of its polarization and spectral index (Reich et al. 1986). According to a recent radio continuum study, the spectral index of this target is 0.23 and there could be a pulsar wind nebula in the central region (Kothes et al. 2006). In HI, Pineault et al. (1996) suggested that there are no obvious HI features associated with the remnant, although large-scale HI features at -45 km s^{-1} indicate a complementary morphology. Case et al. (1998) suggested a distance of 6.6 kpc, based on the $\Sigma - D$ relation.

According to our survey, CO molecular clouds appeared at around +2, -21, and -36 km s^{-1} (Fig. 1). The $+2 \text{ km s}^{-1}$ component was the most prominent (Fig. 2). At this velocity, there is a large and filamentary cloud crossing the northern part of the SNR along east-west direction. The southern part of the SNR is bright in radio continuum, whereas the northern part, where the CO cloud overlaps, is faint. However, there is no evidence of the interaction between the molecular cloud and the SNR. Although we detected a few clumpy clouds at other velocities, they showed no correlation with the SNR.

3.2 G76.9+1.0

This source is the smallest ($\sim 10'$) among our targets. It is a filled-center SNR with a diffuse extended en-

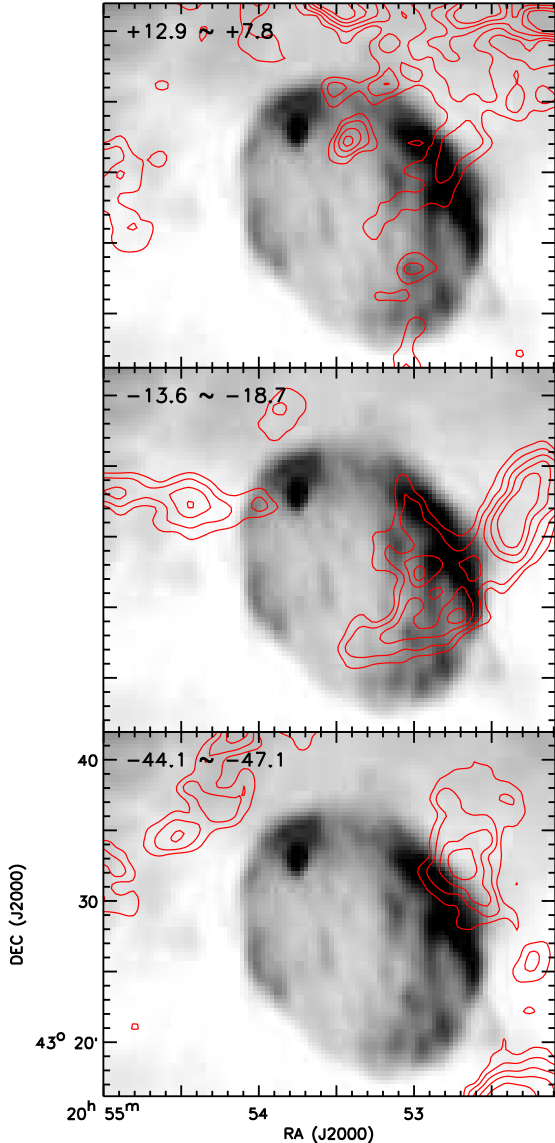


Fig. 4 $^{12}\text{CO } J = 1-0$ average intensity maps of G84.2-0.8 (contour levels: 0.5, 0.8, 1.2, 1.6, 2 K). The gray-scale image is the CGPS 1420 MHz radio continuum image (scale range: 11~24 K).

velope in the radio continuum, and it could be a pulsar wind nebula (Landecker et al. 1993; Kothes et al. 2006). Landecker et al. (1993) suggested a distance greater than 7 kpc based on its large rotation measure. Based on the $\Sigma - D$ relation, Case et al. (1998) estimated the distance to be about 4.7 kpc.

We find that the most prominent CO component that appears at $\sim +5 \text{ km s}^{-1}$ is distributed near the center and the southeast region of the remnant (Figs. 1 & 3). However, this velocity component shows no spatial correlation with the radio continuum. Several CO clouds are also detected around the SNR at a v_{LSR} from -12 to 0 km s^{-1} and near the south-east boundary at

-40 km s^{-1} . However, there is no obvious morphological correlation between the radio and CO distribution.

3.3 G84.2-0.8

G84.2-0.8 is shell-type remnant having filamentary structures parallel to the major axis with no polarized emission (Matthews et al. 1980; Kothes et al. 2006). Huang & Thaddeus (1986) showed that this remnant lied at the south of a large molecular cloud complex at a v_{LSR} between -44 and -33 km s^{-1} . They estimated the kinematic distance to be 7.2 kpc and the total mass to be $8.5 \times 10^5 M_{\odot}$ for the cloud. Feldt & Green (1993) performed $^{12}\text{CO } J = 1-0$ observation with the KOSMA 3-m telescope (FWHM = $3.8'$) in addition to HI observations using the DRAO Synthesis Telescope (FWHM $\approx 1' \times 1.5'$). They found that the CO molecular cloud at -17 km s^{-1} , corresponding to a kinematic distance of ~ 4 kpc is spatially coincident with the SNR. No OH maser emission was detected toward the remnant (Frail et al. 1996).

We detected CO emission at four velocities: $\sim +11$, $+2.7$, -17 , and -46 km s^{-1} (Fig. 1). The -17 km s^{-1} cloud detected by Feldt & Green (1993) is more clearly observed in our data (Fig. 4). There are two clouds: a large one in the west and a small one in the east. The large cloud in the west has a semi-circular shape and is localized inside the remnant. Its northwest boundary matches well with the boundary of the remnant with no asymmetric line emission. The radio continuum is enhanced in the region where a molecular cloud is located. These features suggest a possible interaction between the molecular cloud and the remnant. In order to confirm the interaction, we need to obtain more observations using higher transition CO lines. If this cloud were interacting with the SNR, the distance to the SNR would be 4.9 kpc according to the rotation curve of Brand & Blitz (1993). The velocity component of -46 km s^{-1} appears to be aligned along the southwest and the west. However, it does not show any correlated features with the remnant.

3.4 G85.4+0.7

G85.4+0.7 is shell-type SNR with two separated faint shells, discovered recently from the Canadian Galactic Plane Survey (CGPS) (Kothes et al. 2001a). Kothes et al. (2001a) detected a large HI loop structure surrounding the SNR at a v_{LSR} of -12 km s^{-1} . They interpreted the structure as a stellar-wind shell generated by the progenitor of the SNR, and proposed a distance of 3.8 kpc to the SNR corresponding to the velocity of the HI loop.

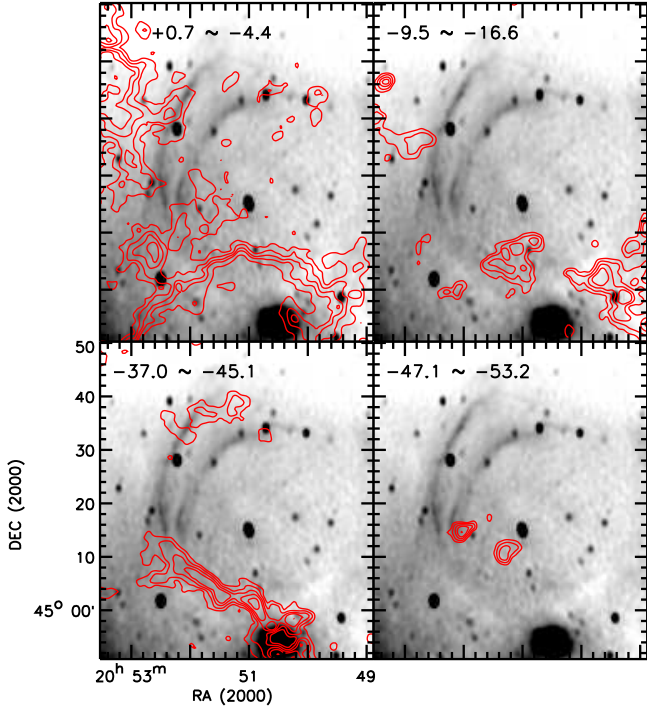


Fig. 5 $^{12}\text{CO } J = 1-0$ average intensity maps of G85.4+0.7 (contour levels: 0.6, 1.0, 1.5, 2, 3 K). The gray-scale image is the CGPS 1420 MHz radio continuum image (scale range: 8.5~11.5 K).

We detected CO emissions at ~ -1 , -12 , -41 , and -50 km s^{-1} (Fig. 1). The molecular cloud at -41 km s^{-1} shows a considerably interesting feature (Fig. 5). This molecular cloud is in filamentary shape and aligned along the south-east boundary of the SNR. The spatial relation between the cloud and the SNR suggests that their association is very likely. The cloud extends to the bright, compact radio source below the remnant, which is the HII region G84.9+0.5 (Foster et al. 2007). The velocity of the HII region from radio recombination line observation is $v_{\text{LSR}} = -39.3 \text{ km s}^{-1}$, and Foster et al. (2007) proposed a kinematic distance of 4.9 kpc considering the noncircular motions near the Perseus spiral arm. The velocity of the CO cloud (-41 km s^{-1}) agrees with that of the radio recombination line, and the cloud surrounds the HII region, which indicates that they are physically associated. The CO emission lines in this area show asymmetric profiles that are probably related to the outflows of young stellar objects. If the -41 km s^{-1} molecular cloud were physically associated with both the HII region and the SNR, the distance to the SNR would be 4.9 kpc (Foster et al. 2007) or 7.2 kpc if we adopt the rotation curve of Brand & Blitz (1993). And it will be difficult to associate the HI loop structure detected by Kothes et al. (2001a) with the SNR. A de-

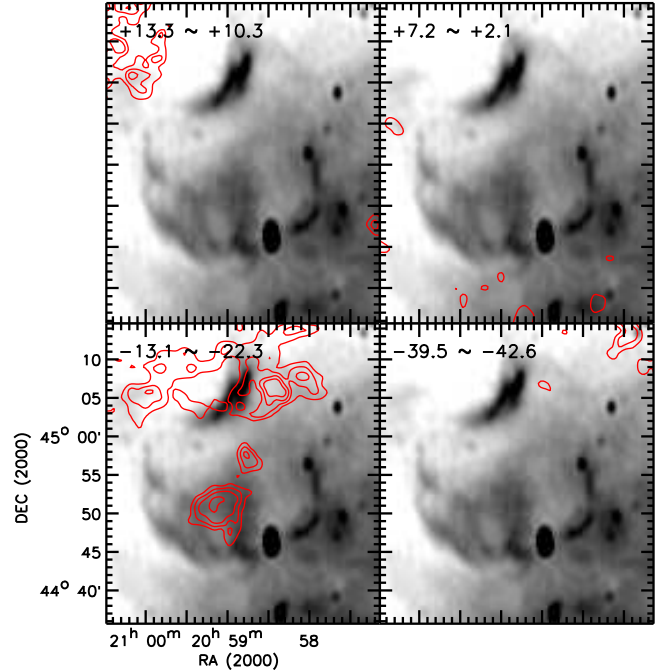


Fig. 6 $^{12}\text{CO } J = 1-0$ average intensity maps of G85.9-0.6 (contour levels: 0.7, 1.1, 1.5, 2 K). The gray-scale image is the CGPS 1420 MHz radio continuum image (scale range: 9.5~14 K).

tailed study on the CO gas and its association with the HII region and the SNR will be presented in a separate paper (Jeong et al. in preparation).

3.5 G85.9-0.6

G85.9-0.6 is a shell-type SNR discovered recently by the CGPS. Kothes et al. (2001a; 2006) suggested that the target might be located in the low-density inter-arm region at $\sim 5 \text{ kpc}$ based on its faint radio and X-ray brightness. There was no particular feature observed from the HI and polarized emission. The distance based on the $\Sigma - D$ relation of Case et al. (1998) is 19.6 kpc.

We detected CO molecular clouds at $+12$, $+5$, -20 , and -41 km s^{-1} (Fig. 1). At -20 km s^{-1} , there is a large molecular cloud near the northern boundary of the SNR and small clouds in the central region of the SNR (Fig. 6). However, there are no indications suggesting the interaction of these clouds with the SNR. The distribution of CO molecular clouds at other velocities does not show any correlation with the radio morphology of the remnant.

3.6 G93.3+6.9 (DA530)

G93.3+6.9 is classified as bilateral type with a well-defined shell morphology in the radio continuum (Gaensler

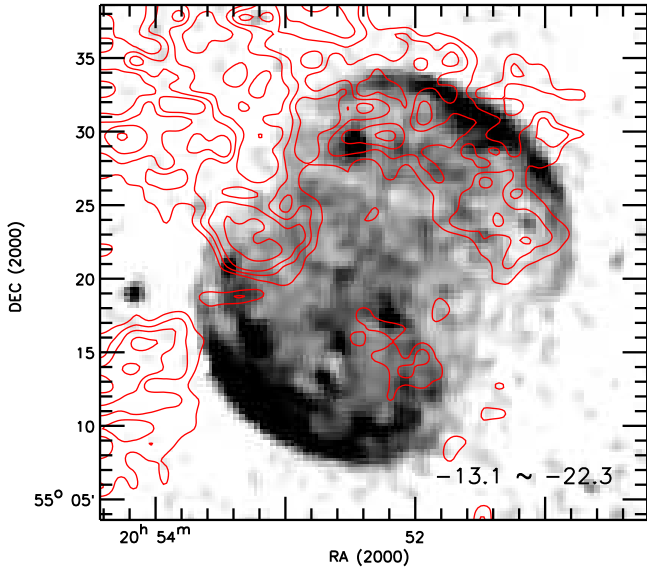


Fig. 7 $^{12}\text{CO } J = 1-0$ average intensity maps of G93.3+6.9 (contour levels: 1.1, 1.3, 1.5, 1.8 K). The gray-scale image is the WENSS 325 MHz radio continuum image (scale range: 9.5~14 Jy/beam) (Rengelink et al. 1990).

1998). This remnant is located at the northern edge of the Cyg OB7 molecular cloud complex at 0.8 kpc that has $v_{\text{LSR}} = -7$ to 0 km s^{-1} (Huang & Thaddeus 1998). Landecker et al. (1999) found an HI bubble at a distance of 3.5 kpc that could have been produced by stellar wind from the massive star progenitor. Foster et al. (2003) estimated the distance of 2.2 kpc by comparing their model of HI column density distribution with the observed HI data. From Chandra X-ray observations, Jiang et al. (2007) found an extended small hard X-ray feature at the centre of the remnant and proposed that it would be pulsar wind nebula. OH maser observation was made toward the remnant with negative results (Frail et al. 1996).

We detected CO emission at -6 to $+5 \text{ km s}^{-1}$ (Fig. 1). Diffuse emissions at $\sim -1.3 \text{ km s}^{-1}$ appear to surround the north-west of the remnant although the morphological correlation between the CO and radio distribution is not clear (Fig. 7).

3.7 G94.0+1.0 (3C434.1)

G94.0+1.0 is a shell type SNR with an asymmetric shape. In radio continuum emission, the western area is faint and has no distinct shell-like feature in visible region, whereas a bright semi-circular shell is evident in the east. In CGPS 1420 MHz radio emission, there was no polarized emission (Willis 1973; Landecker et al. 1985; Kothes et al. 2006). An HI observation suggested that a HI stellar wind bubble at 4.5 kpc is surrounding the remnant and that the progenitor could be an O4

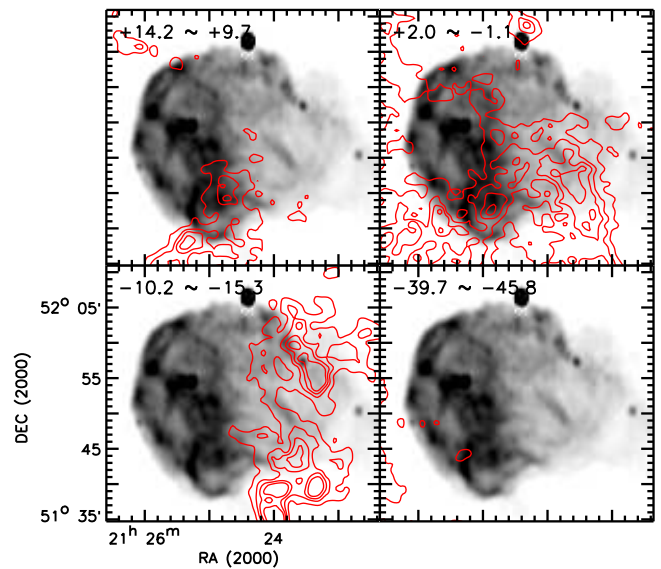


Fig. 8 $^{12}\text{CO } J = 1-0$ average intensity maps of G94.0+1.0 (contour levels: 0.8, 1.5, 2, 2.5 K). The gray-scale image is the CGPS 1420 MHz radio continuum image (scale range: 8~14 K).

star (Foster 2005). By using ROSAT data, he showed that bright, thermal hard X-ray emission was detected toward the radio bright region with good correlation. An OH maser observation was made toward the remnant with negative results (Frail et al. 1996).

We detected molecular gas over a wide velocity range from -70 to -40 km s^{-1} and from -20 to $+20 \text{ km s}^{-1}$ (Fig. 1). The positive velocity components ($v_{\text{LSR}} \geq 0 \text{ km s}^{-1}$) and large negative velocity components ($v_{\text{LSR}} \leq -40 \text{ km s}^{-1}$) do not show any correlated feature between the MCs and the radio continuum emission. We note that there is clear anti-correlation between the CO and radio distribution at $\sim -13 \text{ km s}^{-1}$ (Fig. 8). The large CO cloud is located in the western area of the weak radio continuum region with well-defined spatial correlation. Such anti-correlation is considerably similar to the case of the SNR G109.1-1.0 (CTB109), for which the interaction of the SNR with the molecular cloud occurs (Tatematsu et al. 1987, 1990; Sasaki et al. 2006). A detailed study on the interaction between the molecular cloud and the SNR will be reported in a separate paper (Jeong et al. 2012). If the molecular cloud at -13 km s^{-1} were associated with the SNR, the distance to the SNR would be about 3.0 kpc.

3.8 G166.2+2.5 (OA184)

G166.2+2.5 is a large radio source with low radio surface brightness, and it was known as an evolved SNR (Willis 1973). However, this source has been recently

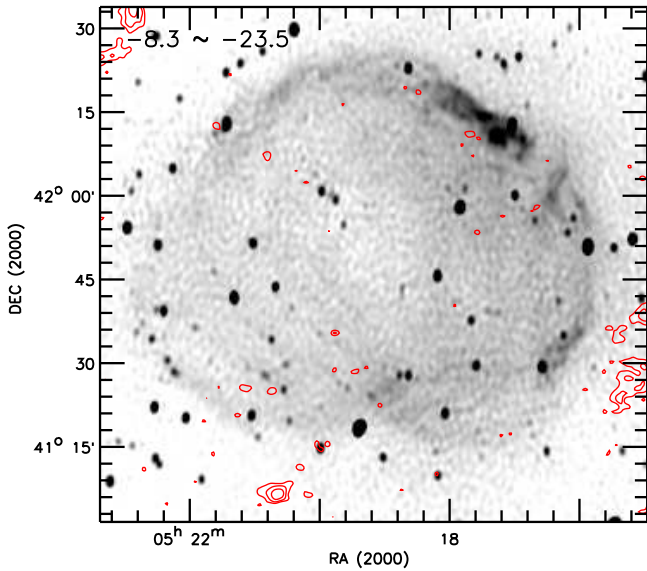


Fig. 9 $^{12}\text{CO } J = 1-0$ average intensity maps of G166.2+2.5 (contour levels: 0.9, 1.3, 1.8 K). The gray-scale image is the CGPS 1420 MHz radio continuum image (scale range: 4.6~6 K).

classified as an HII region based on its flat radio spectral index, missing X-ray emission, and non-significant polarization (Foster et al. 2006). Huang & Thaddeus (1986) noted that OA 184 is located $\sim 2^\circ$ west of VRO 45.05.01 and suggested that both of them are associated with a molecular cloud complex at $v_{\text{LSR}} = -22 \text{ km s}^{-1}$. The cloud complex is located between the two sources and its velocity is coincident with the velocities of the $H\alpha$ emission lines detected toward them (Lozinskaya 1981). Routledge et al. (1986) suggested that an HI feature at a v_{LSR} of -30 km s^{-1} in the southwest is probably associated with the source. OH maser observation was made toward the remnant with a negative result (Frail et al. 1996).

We detected a few small ($\leq 5'$) CO clumps from -26 to -9 km s^{-1} (Fig. 1). These clumps are located $\sim 10'$ away from the radio boundary of the source in the southeast and southwest (Fig. 9). They do not show any correlated features with the remnant.

3.9 G179.0+2.6

G179.0+2.6 is a faint SNR with a diameter of about $70'$. Three bright radio spots near the center of the remnant are radio galaxies along the line of sight (Fuerst et al. 1986; 1989).

CO emission toward this remnant is extremely weak, as shown in Fig. 1. Only one molecular cloud with a $5'$ diameter is detected at $\sim -12 \text{ km s}^{-1}$ (Fig. 10). This cloud lies near the southwest radio boundary; however, no signature of the SNR-MC interaction is observed.

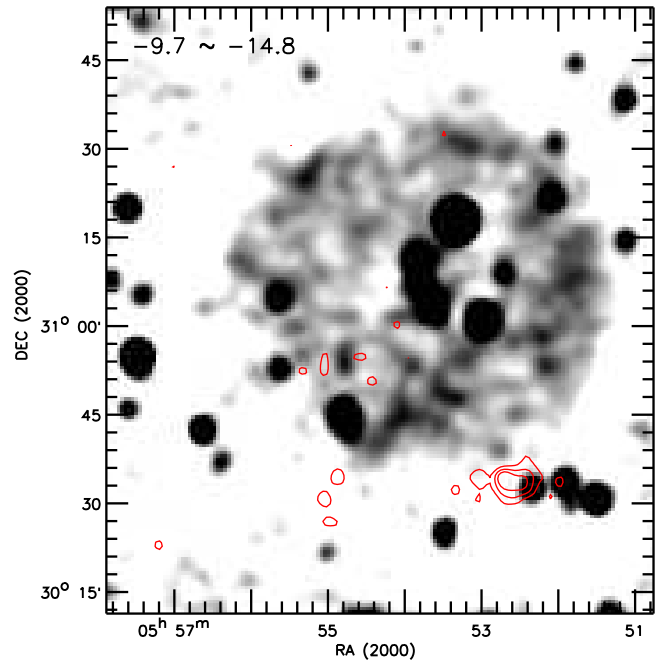


Fig. 10 $^{12}\text{CO } J = 1-0$ average intensity maps of G179.0+2.6 (contour levels: 0.4, 0.8, 1.2 K). The gray-scale image is the WENSS 325 MHz radio continuum image (scale range: 0.5~8 mJy/beam).

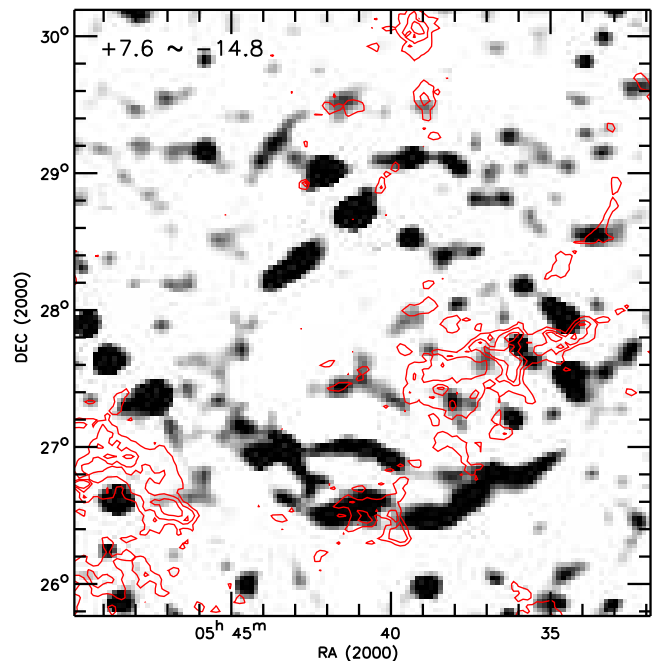


Fig. 11 $^{12}\text{CO } J = 1-0$ average intensity maps of G180.0-1.7 (contour levels: 0.4, 0.8, 1.2 K). The gray-scale image is the GB6 4850 MHz radio continuum image (scale range: 1.7~6.3 mJy/beam) (Condon et al. 1994).

Table 3 Summary of Results

Supernova Remnant	CO velocity ^a (km/s)	Kinematic distance ^b (kpc)	Note
G73.9 +0.9	+3	...	Extended, filamentary MC across the northern part of the remnant along the east-west direction.
G76.9 +1.0	Large cloud across the SNR from southeast to northwest, but no obvious spatially-correlated features.
G84.2 -0.8	-17	4.9	Semi-circular CO cloud coincident with the western SNR boundary with enhanced radio brightness.
G85.4 +0.7	-41	7.2	Long, filamentary MC along the southwestern boundary of the SNR, connected to the compact HII region G84.9+0.5 in the south.
G85.9 -0.6	Several MCs in the field, but no obvious spatially-correlated features.
G93.3 +6.9	-2	...	Large, diffuse MC surrounding the northeast boundary of the SNR.
G94.0 +1.0	-13	3.0	Large molecular clouds blocking the western part of the SNR where the radio emission is faint.
G166.2 +2.5	Several small molecular clumps outside the SNR boundary.
G179.0 +2.6	Small molecular clumps in the southern part of the SNR, but no obvious spatially-correlated features.
G180.0 -1.7	Small MCs in the central area of the SNR without any correlation.
G182.4 +4.3	+4	...	Large, diffuse MC just outside the northwestern boundary of the SNR.

^aVelocity of the CO emission that is spatially-correlated with the SNR.

^bKinematic distances corresponding to the CO velocity assuming the rotation curve of Brand & Blitz (1993). For small CO velocities, no kinematic distances have been derived.

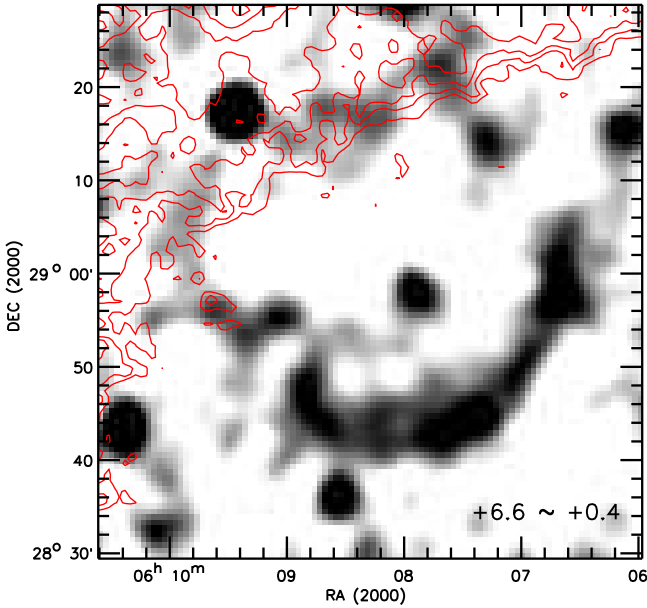


Fig. 12 $^{12}\text{CO } J = 1-0$ average intensity maps of G182.4+4.3 (contour levels: 0.5, 0.8, 1.1, 1.5 K). The gray-scale image is the GB6 4850 MHz radio continuum image (scale range: 0.38~9 mJy/beam).

3.10 G180.0-1.7 (S147)

G180.0-1.7 has large angular size of $\sim 3^\circ$ and remarkable optical filaments (van den Bergh et al. 1973).

Anderson et al. (1996) discovered a pulsar $40'$ away from the center to the west. The age of the pulsar is estimated to be $3 \pm 0.4 \times 10^4$ yr (Kramer et al. 2003). No OH maser emission was detected toward the remnant (Frail et al. 1996).

We found some molecular clouds at velocities from ~ -14 to $+5$ km s^{-1} (Fig. 1). Fig. 11 shows the average intensity map from -14.8 to $+7.6$ km s^{-1} . The cloud at ~ -11 km s^{-1} is located $15'$ away toward the southeast from the radio boundary. CO emission at ~ -5 km s^{-1} is detected near the radio filaments in the south and shows filamentary and clumpy morphology. The cloud at $\sim +1$ km s^{-1} is located in the western part of the remnant where radio brightness is very faint. Although we detected molecular clouds near the SNR, none of them show correlated features with the remnant.

3.11 G182.4+4.3

G182.4+4.3 is a shell-type SNR with a highly polarized, bright partial shell in the southwest (Kothes et al. 1998). The southern shell is bright and circular, whereas the northern shell is faint and flattened. No X-ray emission was detected toward the SNR.

We detected CO emissions at velocities from -9 to $+10$ km s^{-1} (Fig. 1). Most CO emissions arise outside the north and northeast shell of the remnant where the

radio brightness is significantly fainter than that of the south shell. The boundary of the molecular cloud at $\sim +4 \text{ km s}^{-1}$ matches well with the radio boundary of the remnant (Fig. 12). It is possible that the molecular cloud is blocking the remnant, although no direct evidence for their interaction has been detected.

from NASA's *SkyView* and we acknowledge the use of NASA's SkyView facility (<http://skyview.gsfc.nasa.gov>) located at NASA Goddard Space Flight Center.

4 Summary

We carried out $^{12}\text{CO } J = 1-0$ line survey of SNRs using the SRAO 6-m telescope. We observed 11 SNRs between $l = 70^\circ$ and 190° : G73.9+0.9, G76.9+1.0, G84.2-0.8, G85.4+0.7, G85.9-0.6, G93.3+6.9 (DA530), 94.0+1.0 (3C434.1), 166.2+2.5 (OA184), 179.0+2.6, 180.0-1.7 (S147), and G182.4+4.3. The mapping is performed either in half-beam or full-beam sampling to cover the full extents of individual SNRs in the radio continuum. The total number of spectra is about 45,000. We summarize our main results below:

1. We found CO molecular clouds having spatial correlations with radio emission in six SNRs: G73.9+0.9, G84.2-0.8, G85.4+0.7, G93.3+6.9, G94.0+1.0, and G182.4+4.3. However, no strong evidence for the interaction, e.g., broad wings or high-velocity shocked gas, was detected for these objects. We did not detect molecular clouds having any obvious spatial correlation with radio emission in the other SNRs. Table 3 summarizes the results in which the second column lists the velocities of the possibly associated CO features and their kinematic distances. The fourth column gives a short summary on individual SNRs.

2. Two SNRs are particularly interesting. In G85.4+0.7, there is a well-defined filamentary molecular cloud that matches well with the southern boundary of the SNR at -41 km s^{-1} . Another interesting SNR is 3C434.1. It has molecular clouds in the western part of the SNR, where the radio emission is weak. Such anti-correlation between a molecular cloud and radio emission was previously found in the SNR CTB109 (G109.1-1.0), and the their association is likely. Further observations are needed to confirm the interaction between molecular clouds and these SNRs.

Acknowledgements This work is supported in part by the Korean Research Foundation under grant KRF-2008-313-C00372. This research used the facilities of the Canadian Astronomy Data Centre operated by the National Research Council of Canada with the support of the Canadian Space Agency. The GB6 4850 MHz and WENSS 325 MHz radio images were retrieved

References

- Abdo, A.A. et al.: *Astrophys. J. Lett.* **706**, L1 (2009)
- Acciari, V.A. et al.: *Astrophys. J. Lett.* **698**, L133 (2009)
- Aharonian, F. et al.: *Astron. Astrophys.* **490**, 685 (2008)
- Anderson, S.B., Cadwell, B.J., Jacoby, B.A., Wolszczan, A., Foster, R.S., & Kramer, M.: *Astrophys. J.* **468**, L55 (1996)
- Brand, J., & Blitz, L.: *Astron. Astrophys.* **275**, 67 (1993)
- Byun, D.-Y. "Development of the SRAO 6-meter Telescope Control System and Molecular Line Observation of Supernova remnants" PhD thesis, Seoul National University (2004)
- Byun, D.-Y., Koo, B.-C., Tatematsu, K. & Sunada, K.: *Astrophys. J.* **637**, 283 (2006)
- Case, G.L., & Bhattacharya, D.: *Astrophys. J.* **504**, 761 (1998)
- Chen, Y., Su, Y., Slane, P., & Wang, Q. D.: *Astrophys. J.* **616**, 885 (2004)
- Choi, H.-K., Byun, D.-Y., & Koo, B.-C.: *International Journal of Infrared and Millimeter Waves*, **24**, 683 (2003)
- Claussen, M.J., Frail, D.A., Goss, W.M., & Gaume, R.A.: *Astrophys. J.* **489**, 143 (1997)
- Condon, J.J., Broderick, J.J., Seielstad, G.A., Douglas, K. & Gregory, P.C.: *Astron. J.* **107**, 1829 (1994)
- DeNoyer, L.K.: *Astrophys. J. Lett.* **228**, L41 (1979)
- Elitzur, M.: *Astrophys. J.* **203**, 124 (1976)
- Feldt, C., & Green, D.A.: *Astron. Astrophys.* **274**, 421 (1993)
- Foster, T.: *Astron. Astrophys.* **441**, 1043 (2005)
- Foster, T.J., Kothes, R., Kerton, C.R., & Arvidsson, K.: *Astrophys. J.* **667**, 248 (2007)
- Foster, T., Kothes, R., Sun, X.H., Reich, W. & Han, J.L.: *Astron. Astrophys.* **454**, 517 (2006)
- Foster, T., & Routledge, D.: *Astrophys. J.* **598**, 1005 (2003)
- Frail, D.A., Goss, W.M., Reynoso, E.M., Ciacani, E.B., Green, A.J., & Otrupcek, R.: *Astron. J.* **111**, 1651 (1996)
- Fuerst, E., & Reich, W.: *Astron. Astrophys.* **154**, 303 (1986)
- Fuerst, E., Reich, W., Kuhr, H., & Stickel, M.: *Astron. Astrophys.* **223**, 66 (1989)
- Gaensler, B.M.: *Astrophys. J.* **493**, 781 (1998)
- Green, D.A.: *Bulletin of the Astronomical Society of India* **32**, 335 (2004)
- Green, D.A.: *Bulletin of the Astronomical Society of India* **37**, 45 (2009)
- Higgs, L.A., Landecker, T.L. & Roger, R.S.: *Astron. J.* **88**, 97 (1983)
- Huang, Y.-L., & Thaddeus, P.: *Astrophys. J.* **309**, 804 (1986)
- Jackson, J.M. et al.: *Astrophys. J. Suppl. Ser.* **163**, 145 (2006)
- Jeong, I.-G., Koo, B.-C., Cho, W.-K., Kramer, C., Stutzki, J. & Byun, D.-Y.: in preparation (2012)
- Jiang, B., Chen, Y., & Wang, Q.D.: *Astrophys. J.* **670**, 1142 (2007)
- Jiang, B., Chen, Y., Wang, J., Su, Y., Zhou, X., Safi-Harb, S., & DeLaney, T.: *Astrophys. J.* **712**, 1147 (2010)
- Koo, B.-C.: *Shocked Atomic and Molecular Gas in Supernova Remnants* (ASP Conf. Ser. **289**), ed. S. Ikeuchi, J. Hearnshaw, & T. Hanawa (San Francisco: ASP), 199 (2003)
- Koo, B.-C., Park, Y.-S., Hong, S.-S., Yun, H.-S., Lee, S.-G., Byun, D.-Y., Lee, J.-W., Choi, H.-K., Lee, S.-S., Yoon, Y.-Z., Kim, K.-T., Kang, H.-W., & Lee, J.-E.: *JKAS* **36**, 43 (2003)
- Kothes, R., Fedotov, K., Foster, T.J. & Uyaniker, B.: *Astron. Astrophys.* **457**, 1081 (2006)
- Kothes, R., Fuerst, E., & Reich, W.: *Astron. Astrophys.* **331**, 661 (1998)
- Kothes, R., Landecker, T.L., Foster, T., & Leahy, D.A.: *Astron. Astrophys.* **376**, 641 (2001a)
- Kothes, R., Reich, W., Foster, T. & Byun, D.-Y.: *Astrophys. J.* **588**, 852 (2003)
- Kothes, R., Uyaniker, B. & Pineault, S.: *Astrophys. J.* **560**, 236 (2001b)
- Kramer, M., Lyne, A.G., Hobbs, G., Lohmer, O., Carr, P., Jordan, C., & Wolszczan, A.: *Astrophys. J. Lett.* **593**, L31 (2003)
- Landecker, T.L., Higgs, L.A., Roger, R.S.: *Astron. J.* **90**, 1082 (1985)
- Landecker, T.L., Higgs, L.A. & Wendker, H.J.: *Astron. Astrophys.* **276**, 522 (1993)
- Landecker, T.L., Routledge, D., Reynolds, S.P., Smegal, R.J., Borkowski, K.J., & Seward, F.D.: *Astrophys. J.* **527**, 866 (1999)
- Lee, J.-W., Han, S.-T., Byun, D.-Y., Koo, B.-C., & Park, Y.-S.: *International Journal of Infrared and Millimeter Waves* **23**, 47 (2002)
- Lee, J.-J., Koo, B.-C., Snell, R. L., Yun, M. S., Heyer, M. H., & Burton, M. G.: *Astrophys. J.* **749**, 34 (2012)
- Lee, J.-J., Koo, B.-C., Yun, M. S., Stanimirović, S., Heiles, C., & Heyer, M. H.: *Astron. J.* **135**, 796 (2008)
- Lockett, P., Gauthier, E., & Elitzur, M.: *Astrophys. J.* **511**, 235 (1999)
- Lozinskaya, T.A.: *SvAL* **7**, 17 (1981)
- Matthews, H.E. & Shaver, P.A.: *Astron. Astrophys.* **87**, 255 (1980)
- Pineault, S., Gaumont-Guay, S., & Madore, B.: *Astron. J.* **112**, 201 (1996)
- Reich, W., Fuerst, E., Reich, P., Sofue, Y., & Handa, T.: *Astron. Astrophys.* **155**, 185 (1986)
- Reach, W.T. & Rho, J.: *Astrophys. J.* **511**, 836 (1999)
- Rengelink, R.B., Tang, Y., de Bruyn, A.G., Miley, G.K., Bremer, M.N., Roettgering, H.J.A. & Bremer, M.A.R.: *Astron. Astrophys. Suppl. Ser.* **124**, 259 (1997)
- Routledge, D., Landecker, T.L., & Vaneldik, J.F.: *Mon. Not. R. Astron. Soc.* **221**, 809 (1986)
- Sasaki, M., Kothes, R., Plucinsky, P.P., Gaetz, T.J. & Brunt, C.M.: *Astrophys. J. Lett.* **642**, L149 (2006)
- Snell, R.L., Hollenbach, D., Howe, J.E., Neufeld, D.A., Kaufman, M.J., Melnick, G.J., Bergin, E.A., & Wang, Z.: *Astrophys. J.* **620**, 758 (2005)
- Tatematsu, K., Fukui, Y., Iwata, T., Seward, F.- D., & Nakano, M.: *Astrophys. J.* **351**, 157 (1990)
- Tatematsu, K., Fukui, Y., Nakano, M., Kogure, T., Ogawa, H. & Kawabata, K.: *Astron. Astrophys.* **184**, 279 (1987)
- Taylor, A.R., et al.: *Astron. J.* **125**, 3145 (2003)
- van den Bergh, S., Marscher, A.P., & Terzian, Y.: *Astrophys. J. Suppl. Ser.* **26**, 19 (1973)
- Wardle, M.: *Astrophys. J.* **525**, L101 (1999)
- Wardle, M., & Yusef-Zadeh, F.: *Science* **296**, 2350 (2002)
- Willis, A.G.: *Astron. Astrophys.* **26**, 237 (1973)